



Deposited via The University of Leeds.

White Rose Research Online URL for this paper:

<https://eprints.whiterose.ac.uk/id/eprint/88956/>

Version: Published Version

Article:

Forth, JP, Ru, M, Scott, R et al. (2013) Verification of shrinkage curvature code prediction models. *ICE Structures and Buildings*, 167 (5). 274 - 284. ISSN: 0965-0911

<https://doi.org/10.1680/stbu.12.00046>

Reuse

Items deposited in White Rose Research Online are protected by copyright, with all rights reserved unless indicated otherwise. They may be downloaded and/or printed for private study, or other acts as permitted by national copyright laws. The publisher or other rights holders may allow further reproduction and re-use of the full text version. This is indicated by the licence information on the White Rose Research Online record for the item.

Takedown

If you consider content in White Rose Research Online to be in breach of UK law, please notify us by emailing eprints@whiterose.ac.uk including the URL of the record and the reason for the withdrawal request.

Verification of cracked section shrinkage curvature models

- 1 John P. Forth** PhD, CEng, MStructE
Senior Lecturer, School of Civil Engineering, University of Leeds, Leeds, UK
- 2 Ru Mu** PhD
Senior Engineer, School of Civil Engineering, Hebei University of Technology, Tianjin, China
- 3 Richard H. Scott** MSc, DIC, PhD, CEng, MICE, FStructE
Visiting Professor in Structural Engineering, School of Engineering and Mathematical Sciences, City University London, London, UK
- 4 Anthony E. K. Jones** PhD, CEng, FICE, FStructE
Associate Director, Arup, London, UK
- 5 Andrew W. Beeby** PhD, FEng, CEng, MICE, FStructE, FFB, FAcI
Emeritus Professor, School of Civil Engineering, University of Leeds, Leeds, UK



An attempt is made to theoretically and experimentally verify the shrinkage curvature models presented in Eurocode 2 and BS 8110. These codes claim that the models originally derived and proven for uncracked sections are suitable, with modification, for predicting the behaviour of cracked sections, although this claim has never been proven experimentally. To achieve verification, an alternative theoretical approach is initially proposed in this paper. In this theoretical model, the effect of shrinkage, creep and the variation in the neutral axis position of the section are taken into account. The stresses developed in the steel and concrete at a cracked section according to this theoretical model are then applied to a finite-element (FE) model representing a portion of the beam from the crack to mid-way between the crack and an adjacent crack. Ultimately, the mean curvature is determined. Experimentally, pairs of beams were cast and subjected to a level of flexural loading to produce a stabilised crack pattern in the constant-moment zone. The behaviour of the beams was monitored for up to 180 days. For any pair of beams, one beam was cast using a high-shrinkage concrete and the other with a low-shrinkage concrete. Each concrete type, however, exhibits similar creep. Therefore, shrinkage curvature can be obtained by subtracting the long-term movements of one beam from the other. These experimentally defined curvatures were compared with the mean curvatures obtained from the FE analysis. The comparison showed reasonable agreement. The curvatures were also compared with uncracked and cracked curvatures predicted by the codes. The curvatures derived in this investigation fell within the boundaries of the uncracked and cracked curvatures predicted by the codes and, for the fully cracked case, the curvatures were closer to the uncracked boundary.

Notation

A_c	area of concrete		
A_s	area of tension reinforcement	M	of an age-adjusted transformed section (Equation 5)
A'_s	area of compression reinforcement		external applied bending moment
C	cover depth	N	sum of normal forces
d, d'	depth of tensile and compressive reinforcement respectively (Equation 4)	$1/r_{cs}$	shrinkage curvature
E_c	elastic modulus of concrete at the time of estimation	r_c^2	$= I_c/A_c$, A_c and I_c being the area of the compression zone and its moment of inertia about an axis through the centroid of the section (Equation 5)
E_s	Young's modulus of reinforcement (Equation 4)	S	first moment of area of the reinforcement about the centroid of the cracked or gross section
h	height of the section	$2S_0$	theoretical crack spacing
I	second moment of area of the cracked or gross section	t_0	age at loading
\bar{I}	moment of inertia about an axis through the centroid	t_1, t_2	time intervals

x	depth of neutral axis (Equation 4)
y_c	y -coordinate of the centroid of the concrete area in compression (based on the stress distribution at age t_0) (Equation 5)
y_s	distance to bottom steel from whatever axis is chosen
y'_s	distance to the top steel from whatever axis is chosen
α	deformation parameter considered (e.g. a strain, a curvature or a rotation)
α_I, α_{II}	values of parameters calculated for uncracked and fully cracked conditions respectively
α_e	modular ratio
β	coefficient taking account of the influence of the duration of the loading or of repeated loading on the average strain
δh	height of individual strip
ε_{cs}	free shrinkage strain
$\varepsilon_{cs}(t, t_0)$	shrinkage that would occur in the concrete if it were free, during the period $t - t_0$ (Equation 5)
ε_{sh}	shrinkage of concrete
ε_{tot}	total strain of concrete
ζ	distribution coefficient (allowing for tensioning stiffening at a section)
κ	curvature reduction factor ($= I_c / \bar{I}$) (Equation 5)
σ_1, σ_2	stress applied at t_1, t_2
σ_c	stress in concrete
σ_s	stress in tension reinforcement calculated on the basis of a cracked section
σ_{sr}	stress in tension reinforcement calculated on the basis of a cracked section under the loading conditions causing first cracking
σ'_s	stress in top steel
ϕ	creep coefficient of concrete
ψ	creep coefficient of concrete in Equation 4

1. Introduction

The first step in design is usually to perform ultimate limit state analysis; the serviceability limit state is then verified. In many cases, however, serviceability (i.e. deflection) is critical and it is this limit state for which the section, reinforcement and even the materials are determined. As the properties of concrete, typically shrinkage, develop with age, the serviceability of a concrete element is affected – it will behave time dependently. The effect of shrinkage on the deformation of concrete beams was investigated both theoretically and experimentally as far back as the 1970s (Hobbs, 1979) and conclusions from such investigations have been included in structural design codes such as BS 8110 (BSI, 1985) and Eurocode 2 (EC2) (BSI, 2004).

In BS 8110, Equation 1 is recommended to calculate the curvature of uncracked or cracked spanning elements caused by shrinkage of concrete

$$1. \quad \frac{1}{r_{cs}} = \alpha \varepsilon_{cs} \left(\frac{S}{I} \right)$$

where $1/r_{cs}$ is shrinkage curvature, ε_{cs} is the free shrinkage strain, α_e is the modular ratio, S is the first moment of area of the reinforcement about the centroid of the cracked or gross section and I is the second moment of area of the cracked or gross section. However, as noted in earlier work (Mu *et al.*, 2008), derivation of this equation was based on an uncracked section (BSI, 1985: section 3.6).

Similarly, an uncracked section derived equation is suggested to predict shrinkage curvature in EC2 (BSI, 2004: section 7.4.3). However, in an attempt to recognise that the mean curvature of a beam or slab will lie somewhere between the curvature predicted at a cracked and uncracked section, depending on the degree of cracking (or, for instance, the ratio of cracking moment to applied moment), EC2 also recommends a universal equation for the prediction of the average value of the deformation parameters, including curvature, of cracked beams (BSI, 2004: section 7.4.3)

$$2. \quad \alpha = \zeta \alpha_{II} + (1 - \zeta) \alpha_I$$

where α is the deformation parameter considered (which may be, for example, a strain, a curvature or a rotation), α_I and α_{II} are the values of the parameter calculated for the uncracked and fully cracked conditions respectively and ζ is a distribution coefficient (allowing for tensioning stiffening at a section) given by

$$3. \quad \zeta = 1 - \beta \left(\frac{\sigma_{sr}}{\sigma_s} \right)^2$$

where $\zeta = 0$ for uncracked sections. β is a coefficient taking account of the influence of the duration of the loading or of repeated loading on the average strain ($\beta = 1.0$ for a single short-term loading and $\beta = 0.5$ for sustained loads or many cycles of repeated loading), σ_s is the stress in the tension reinforcement calculated on the basis of a cracked section and σ_{sr} is the stress in the tension reinforcement calculated on the basis of a cracked section under the loading conditions causing first cracking.

Equation 1, which is adopted in the two codes, although originally derived for uncracked sections, is suggested by the codes to be applicable to cracked sections. However, this guidance has never been proven theoretically, nor has it been experimentally validated.

The shrinkage curvature model proposed by Hobbs (Hobbs, 1979) is given as Equation 4 and, again, was originally derived for an uncracked section. The equation is effectively the same as Equation 1. Hobbs also suggested that this formula was suitable for calculation of the shrinkage curvature of cracked sections

$$4. \quad \frac{1}{r_{cs}} = \frac{(1 + \psi)\varepsilon_{cs}E_s[A_s(d - x) - A'_s(x - d')]}{E_c I}$$

in which ε_{cs} is the shrinkage that would occur in concrete if it were unrestrained, ψ is the creep coefficient of concrete, E_s is Young's modulus of the reinforcement, E_c is Young's modulus of concrete, I is the moment of inertia of the cracked or uncracked section about an axis through the centroid of an age-adjusted transformed section, x is the depth of neutral axis and d and d' are the depth of tensile and compressive reinforcement respectively.

Another model for the prediction of the shrinkage curvature of sections fully cracked due to an external applied bending moment has been developed (Ghali and Favre, 1986) and is shown as Equation 5. As with the previous examples, this is an approximated model; that is, besides the common assumption that plane sections remain plane, a fixed neutral axis position assumption was adopted in the derivation of Equation 5, irrespective of shrinkage

$$5. \quad \frac{1}{r_{cs}} = \kappa \varepsilon_{cs}(t, t_0) \frac{y_c}{r_c^2}$$

where $\varepsilon_{cs}(t, t_0)$ is the shrinkage that would occur in the concrete if it were free, during the period $t - t_0$, $r_c^2 = I_c/A_c$ (A_c and I_c being respectively the area of the compression zone and its moment of inertia about an axis through the centroid of the section), κ is the curvature reduction factor ($= I_c/\bar{I}$; \bar{I} being the moment of inertia about an axis through the centroid of an age-adjusted transformed section), y_c is the y -coordinate of the centroid of the concrete area in compression (based on the stress distribution at age t_0) and M is the external applied bending moment.

Shrinkage and creep of concrete always result in a significant shift in the position of the neutral axis towards the tensile area of the section, so fixing the neutral axis position will affect the accuracy of the prediction. However, based on the analysis presented later in Section 3, the predictions are not too dissimilar to the previously acceptable code guidance (BS 8110 model).

In this paper, an attempt is made to validate the mean shrinkage curvatures predicted by the models in the codes for a fully cracked section (i.e. Equations 1 and (2) and even Equation 4), using experimentally defined shrinkage curvatures and curvatures predicted using a new theoretical approach (combined with finite-element (FE) analysis).

2. Theoretical approach for curvature calculation

To theoretically validate the existing shrinkage curvature models, an alternative methodology is proposed. The proposed approach

avoids the oversimplification in the current code derivations that could potentially significantly affect the accuracy of the analysis. The approach is based on common cross-sectional analysis and the effective modulus method developed by Faber (1927). A Matlab programme, utilising existing theories, was then developed to determine the shrinkage curvature.

Consider a simply supported rectangular section beam with both top and bottom reinforcement. The beam is fully cracked due to an external applied positive bending moment M introduced at age t_0 and kept constant. The analysis concerns a section at a crack. As with the majority of methodologies, a series of assumptions and simplifications are employed. The two basic assumptions adopted in this current analysis are as follows

- plane sections remain plane
- creep is linear (i.e. creep strain is proportional to stress) (Favre *et al.*, 1983).

Assume that cracking occurs instantly immediately after the load is applied and the concrete has zero initial shrinkage and creep. Further, assume the concrete has zero tensile strength, meaning that the tension zone is ineffective at resisting any forces. Immediately after the load is applied when no shrinkage or creep have occurred, the elastic curvature of the cracked section can be calculated using Equation 6 and the other properties of the section, such as the neutral axis position and the stress and strain of the section, can be determined easily from mechanical equilibrium equations

$$6. \quad \frac{1}{r} = \frac{M}{EI}$$

Here, I is the moment of inertia of the transformed section, composed of αA_s , $\alpha A'_s$ and A_c , about the centroidal axis (which is the same as the neutral axis), M is the external applied moment and E is the elastic modulus of concrete.

At age t_1 , some shrinkage and creep have taken place, leading to a change in the neutral axis position of the section, and Equation 6, as explained below, is no longer suitable for the analysis of the section. To identify the new position of the neutral axis, an approximation approach is developed, in which the shrinkage, creep and the shift of neutral axis position are considered and equated. In the approximation, the cross-section is divided horizontally into a number of strips and the state of each strip is analysed. Then, the load over the section is obtained by integrating the loads on all the strips, which should equal the external load applied to the section. Finally, by iteration, the true stress and strain of each strip, the real neutral axis position and hence the curvature of the section are determined. Although this is an approximation, the greater the number of strips, the more accurate will be the result. Therefore, in theory, greater precision of results could be achieved by using even finer strips. Details of the theoretical analysis are now described.

2.1 Equilibration conditions

Figure 1 illustrates the cross-section, which is divided into strips with height δh . First of all, the values for the neutral axis position x and the curvature $1/r$ are estimated. The average strain and hence the average stress in each strip can then be calculated. Finally, the strains and hence the stresses in the top and bottom steel can be calculated. By equilibrium

$$7. \quad A'_s \sigma'_s + A_s \sigma_s + \sum \sigma_i b \delta h = N = 0$$

$$8. \quad A'_s \sigma'_s y'_s + A_s \sigma_s y_s + \sum \sigma_i b \delta h y_i = M$$

where σ'_s is the stress in top steel, σ_s is the stress in bottom steel, σ_i is the stress in the i th strip, y'_s is the distance to the top steel from whatever axis is chosen, y_s is the distance to the bottom steel from whatever axis is chosen and y_i is the distance to the centre of the i th strip from whatever axis is chosen.

As no external axial force is applied, the sum of the normal forces of all strips and reinforcement N , which is the left-hand side of Equation 7, equals zero. At this stage, the tensile strength of concrete is assumed to be zero and tension stiffening is ignored. So, the concrete stress will be zero in any strip wholly within the tension zone. The tensile strength of the concrete may be considered in the future when necessary.

Using the initial estimates for curvature and neutral axis position, if either or both Equations 7 or 8 are untrue, then the values of x and/or $1/r$ are adjusted and equilibrium is checked again. When both equations are satisfied, the correct values of x and $1/r$ have been found and the analysis is complete. To obtain the correct answer in relatively few cycles, the relationship between the two incremental variables (i.e. changes in curvature and neutral axis position) and the corresponding increase in bending moment and axial force can be manually derived. Conversely, using this

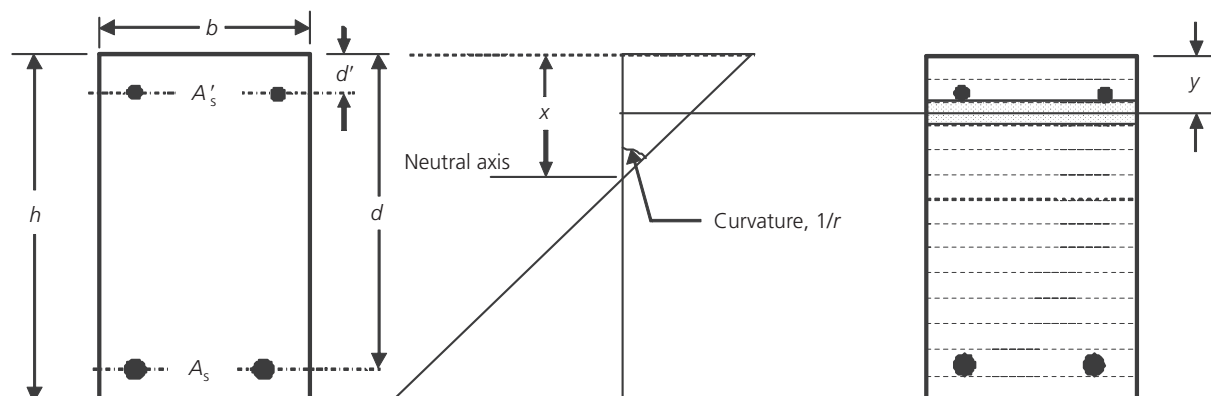


Figure 1. Sketch of cross-section and strain

relationship, by setting the increase in force and moment to the necessary values to meet the equilibrium condition of Equations 7 and 8, the appropriate adjustment of x and $1/r$ can be obtained.

2.2 Effects of shrinkage and creep

In Equations 7 and 8, the effects of shrinkage and creep are incorporated when the stress of the strips is calculated from the strain. Creep and shrinkage are treated as independent phenomena with no interaction; this is a normal assumption in design calculations, but by no means necessarily true.

2.2.1 Effect of shrinkage

By considering the effect of shrinkage, the stress–strain relationship of concrete becomes

$$9. \quad \sigma_c = (\epsilon_{\text{tot}} - \epsilon_{\text{sh}}) E_c$$

where σ_c is the stress in concrete, ϵ_{tot} is the total strain of concrete, ϵ_{sh} is the shrinkage of concrete and E_c is the elastic modulus of the concrete at the time of estimation.

The shrinkage influences not only the stress–strain relationship but also the neutral axis position of the section as schematically shown in Figure 2. The shrinking of concrete results in the neutral axis position moving downwards.

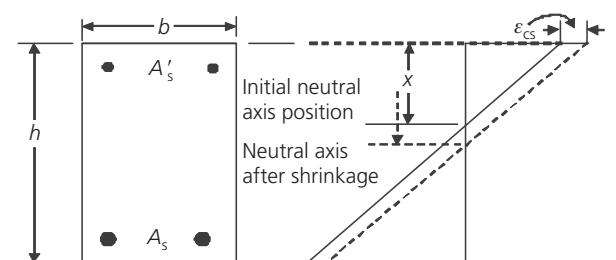


Figure 2. Effect of shrinkage on neutral axis position

2.2.2 Effect of creep

In the stress–strain relationship, the effect of creep can be considered by incorporating a creep coefficient ϕ

$$10. \quad \sigma_c = E_c \varepsilon_{\text{tot}} \left(\frac{1}{1 + \phi} \right)$$

where ε_{tot} is the total strain of the concrete.

For analysis of a section of a purely bending beam, however, Equation 10 cannot be used directly because the stress within the cross-section varies with time even though the bending moment may be constant. An approximation is made to simplify the analysis, as shown in Figure 3. As can be seen, the variation in stress is gradual. However, in order to develop the analysis, it is assumed that the change in stress occurs instantaneously and is equivalent to a new stress ($\delta\sigma_i$) being applied at the end of each time step. In this way, the stresses are considered constant for each time step, but new stresses are applied continuously. Incorporating the assumption of linear creep, stress with consideration of creep can be analysed.

Figure 4 illustrates an element close to the compression face and hence all $\delta\sigma$ values are negative. Creep is assumed to occur only due to the stress σ_0 from t_0 to t_1 , and due to the stress σ_1 from t_1

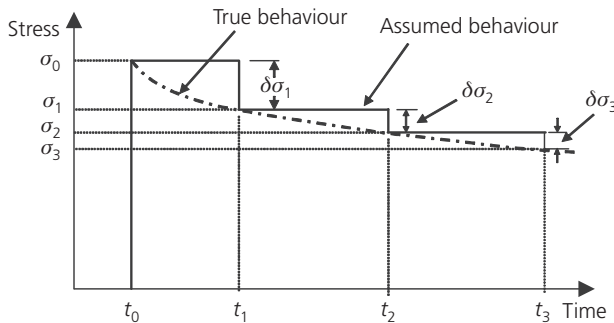


Figure 3. Approximation of stress behaviour

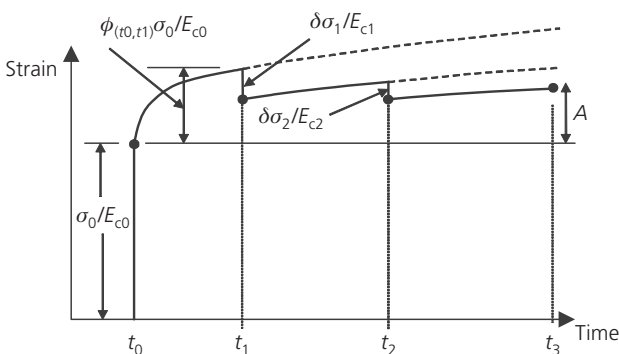


Figure 4. Sketch of superposition of creep

to t_2 and so on. It is assumed that the creep from each increment in stress can be superposed and thus deformations can be assumed to develop.

In the sketch of Figure 4, the long-term increment in strain at time t_3 (A) is given by

$$11. \quad A = \frac{\phi_{(t_0,t_3)}\sigma_0}{E_{c0}} + \frac{\delta\sigma_1}{E_{c1}} + \frac{\phi_{(t_1,t_3)}\delta\sigma_1}{E_{c1}} + \frac{\delta\sigma_2}{E_{c2}} + \frac{\phi_{(t_2,t_3)}\delta\sigma_2}{E_{c2}} + \frac{\delta\sigma_3}{E_{c3}}$$

The total strain can now be expressed as

$$12. \quad \varepsilon_3 = \frac{(1 + \phi_{(t_0,t_3)})\sigma_0}{E_{c0}} + \frac{(1 + \phi_{(t_1,t_3)})\delta\sigma_1}{E_{c1}} + \frac{(1 + \phi_{(t_2,t_3)})\delta\sigma_2}{E_{c2}} + \frac{\delta\sigma_3}{E_{c3}} + \varepsilon_{\text{sh}(t_i,t_3)}$$

where $\varepsilon_{\text{sh}(t_i,t_3)}$ is the shrinkage from the time of the start of drying (t_i) to t_3 .

Clearly, this form of calculation can be extended to any time t_n , even time step t_0 immediately after the load is applied but when no shrinkage or creep has taken place. To validate this approach, the first step of the analysis immediately after loading was performed and the output checked with that from Equation 6. It was confirmed that the new method gave the same result as Equation 6. This approach can also be applied to uncracked sections; the only necessary change is that the stress of the strips in the tension area is not taken as zero.

Based on the approach described above, a Matlab programme was developed. Using the programme, the neutral axis position, curvature of the cracked sections, and the stress and strain of the concrete and reinforcement in any section can be determined. The effect of shrinkage on beam curvatures can be investigated by making a comparison between the analytical curvatures of two beams with different shrinkage.

To perform the analysis, models for the variation in elastic modulus, strength, creep coefficient and free shrinkage as functions of time are required. These were obtained from the equations given in EC2 (BSI, 2004) (and cross-checked with measured data recorded as part of this investigation). In the shrinkage and creep models, the relative humidity and temperature were assumed to remain constant.

3. Verification of code-predicted cracked section shrinkage curvatures

Consider a cracked section, 300 mm wide and 150 mm deep, subjected to a pure bending moment 12.5×10^3 kN m. The section is reinforced with 3T16 bottom bars and 2T10 top bars. The clear cover depth (reinforcement surface to concrete surface) is 30 mm. The compressive strength of the concrete is 54 MPa at 28 days. The strength, shrinkage and creep were determined using the relevant models given in EC2 as functions of time. Figure 5 shows two shrinkage curves (high shrinkage and low shrinkage) generated using the shrinkage model in EC2 with different parameters, which will be used as input for the model analysis. The relative humidity and temperature are assumed to be constant at 60% and 21°C respectively over the duration considered.

3.1 Shrinkage curvature

Figure 6 shows the analysis results for the curvatures of sections with high and low shrinkage. The curvatures of both sections

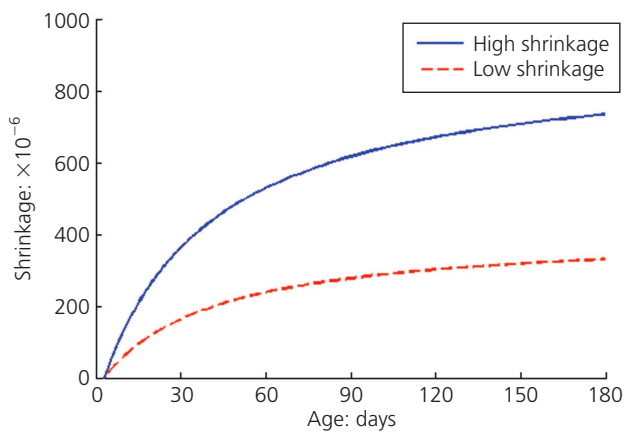


Figure 5. Shrinkage of two concretes

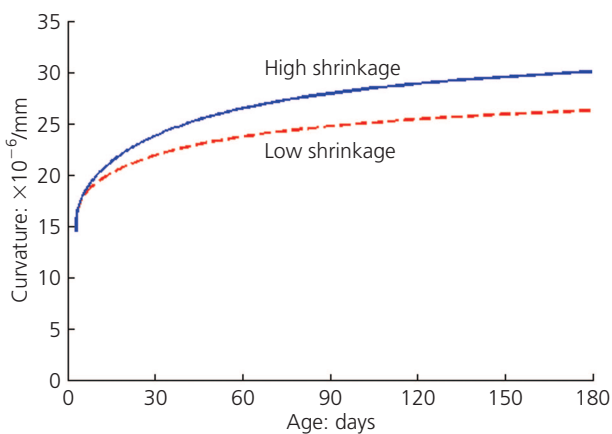


Figure 6. Curvature of cracked section with high- and low-shrinkage concrete (high shrinkage, $14.507\text{--}30.052 \times 10^{-6}/\text{mm}$; low shrinkage, $14.507\text{--}26.269 \times 10^{-6}/\text{mm}$)

increase with time due to the shrinkage and creep of concrete. However, the curvature of the high-shrinkage section grows more quickly than that of the low-shrinkage section; this is purely due to the shrinkage because all other inputs, including creep, for the two sections are the same. The difference in curvature between the two curves is thus the shrinkage curvature, and is plotted in Figure 7(a) along with shrinkage curvatures from the BS 8110 model and the models of Hobbs (1979) and Ghali and Favre (1986) for cracked sections.

In Figure 7(a), the input in creating the shrinkage curvatures from the models of BS 8110, Hobbs, and Ghali and Favre is 'clear shrinkage', which is the high shrinkage minus the low shrinkage in Figure 5. It can be seen that the shrinkage curvature from the Hobbs model is about three times that from the other models. The curvature of the Ghali and Favre model is about 15% higher than the proposed ('New') and BS 8110 models, which is because of the assumption of a fixed neutral axis position in Ghali and Favre's model. The much higher prediction of the Hobbs model is

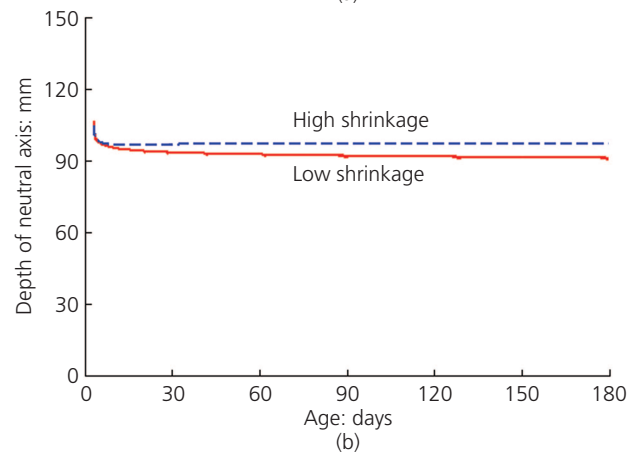
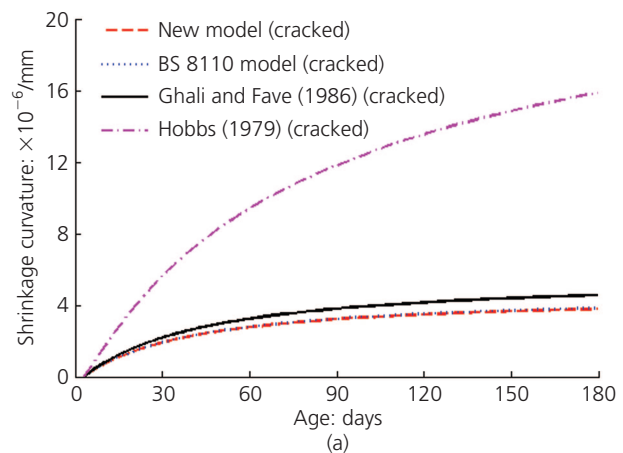


Figure 7. (a) Comparison of shrinkage curvature of cracked section. (b) Neutral axis position of section at crack (high shrinkage, 106.5–97.0 mm; low shrinkage, 106.5–90.5 mm)

because the effective modulus is adopted in the calculation of the second moment of the section whereas, in the other models, the effective modulus is used to determine the area of transformed section only. The prediction of shrinkage curvature using the EC2/BS 8110 model (Equation 1) is almost the same as the new method proposed in this paper. In Equation 1, the effect of applying the shrinkage later is to reduce the modular ratio (α_e), reduce I and slightly increase S . These changes almost exactly balance each other with the result that the shrinkage curvature is accidentally unaffected.

3.2 Neutral axis position

Using the iteration method proposed in Section 2, the neutral axis position of the cracked section against time was determined (Figure 7(b)). The shrinkage input for the neutral axis depth calculation is that in Figure 5. As can be seen from Figure 7(b), for a 150 mm high, 300 mm wide section under bending moment load applied at age 3 days, the neutral axis position of the section falls from 106.5 mm immediately after load application to 97.0 mm (for high shrinkage) or 90.5 mm (for low shrinkage) at age 180 days. This change can significantly influence the properties of the section, especially its moment of inertia, which obviously has an influence on the curvature of the section under bending.

4. Experimental validation

The proposed shrinkage curvature approach was validated via experiments. Experimentally, the major difficulty has always been separating the influences of shrinkage and creep on curvature. To overcome this problem, two concrete mixes were designed – one with low shrinkage and one with high shrinkage – but with similar creep. Two beams were then cast with each mix and loaded to produce stabilised crack patterns. Any difference in curvature between the two beams is, therefore, due to shrinkage. Once this was achieved, comparisons were made between the experimental tests and the predictions using the proposed modelling approach.

4.1 Details of experimental tests

The dimension and reinforcement details of the beams are given in Figure 8(a); the beams were 150 mm deep, 300 mm wide and 4200 mm long. The cover depth (from concrete surface to bar surface) was 30 mm. No link reinforcement was placed in the constant-moment zone. The beam pair is denoted B2.

After casting, the beams were cured in moulds covered with wet burlap and plastic sheeting until they were loaded at an age of 3 days. Companion prisms to obtain creep and free shrinkage data for the mixes and cubes for compressive strength tests were cast

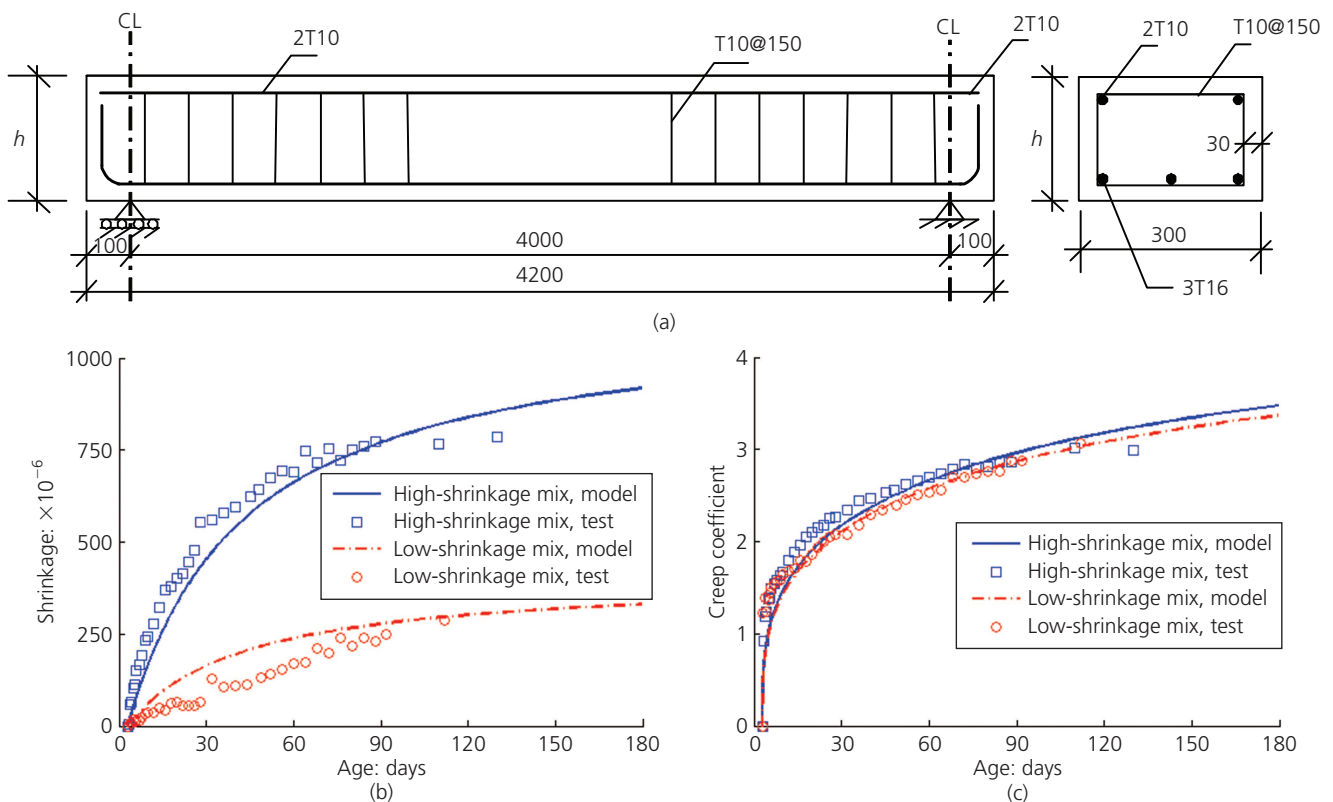


Figure 8. (a) Details of reinforcement of concrete beams (dimensions in mm). (b) Shrinkage plotted against time. (c) Creep coefficient plotted against time

from the mixes used for the beams. They were also cured in the same way. Figures 8(b) and 8(c) respectively illustrate the shrinkage and creep coefficients of the high- and low-shrinkage prism mixes. Also shown in the figures are the long-term movement predictions using MC90 (FIB, 1993).

Three days after casting, the beams were demoulded and placed in the test rigs. A four-point bending load was applied to the beams. The span of the beams was 4000 mm and the two loading points were 1500 mm apart. At each loading point, a load of 18 kN was applied by a hydraulic jack. A stabilised crack pattern was achieved (confirmed by analytical checks). The load was monitored and adjusted frequently to ensure that it remained constant. The ambient temperature in the laboratory was in the range 20–25°C and the relative humidity was 40–60%.

In order to monitor the curvature and the depth of neutral axis with time, Demec gauges (200 mm) were used to measure the horizontal strain on the side of the beam in the region of the constant-moment zone. The strain was measured at four different depths, two of which corresponded to the position of the main tensile and compressive reinforcement; the other two were equally spaced between the two lines corresponding to the reinforcement position. Readings were taken twice daily for the first 2 days. The frequency of readings was then reduced to once per day, then once every 2 days and finally once every 4 days after the age of 5 days, 3 weeks and 6 weeks respectively. Although the stress in the tension concrete is not considered for a fully cracked beam, shrinkage and creep of the concrete in tension do occur (as shown by the Demec measurements in the tension zone), which may slightly influence the stress in concrete. Furthermore, taking an average of the Demec strains for the four Demec lines on the side of the beams and checking the strains down through the depth, it was found that the plane section assumption is correct.

From the test readings, the total curvature and neutral axis depths of the two beams could be determined. The shrinkage curvature, which is (as explained earlier) the difference in curvature between the two beams, could therefore be calculated. The shrinkage curvature from the tests represents the mean curvature value over the constant-moment portion of the beams. However, the curvature predicted by the theoretical model is the curvature of a section either at a crack or mid-way between any two adjacent cracks (uncracked section). What the new theoretical approach does not do (as is the case with any of the other current prediction methods) is predict the curvature of a section near a crack (i.e. a section in the region between the crack and half-way between two adjacent cracks). In this region, although the section is uncracked, its behaviour will be influenced by the crack. To obtain the curvature in the region where a section is influenced by the crack, FE analysis was performed. The refinement of the new theoretical approach using the FE analysis is described in the next section – the curvature obtained using the FE analysis represents the mean curvature for the constant-moment zone.

4.2 Mean shrinkage curvature using FE analysis

For the fully cracked beam under constant bending, an FE model can be developed to represent that part of the beam from the crack to mid-way between two adjacent cracks. In theory, this represents all parts of the beam within the constant-moment zone. According to research by Beeby and Scott (2004), it is reasonable to assume that the average crack spacing of a fully cracked beam is two-thirds of the theoretical crack spacing $2S_0$, where $S_0 = 3.0C$ (Beeby and Scott, 2004), C being the cover depth of the reinforcement. The cover depth in the model and the tests was 30 mm (or 38 mm from the centroid of the section of rebar to the concrete surface) and hence the average crack spacing is 120 mm or 152 mm. So, half the crack spacing is somewhere between 60 and 76 mm. Therefore, a 70 mm wide portion of the beam was adopted in the FE analysis, as shown in Figure 9.

In the FE analysis, one vertical face corresponds to the mid-point section between two adjacent cracks; the concrete between two adjacent cracks is symmetrical about this vertical face and is, therefore, considered as ‘fixed’ in the model. The other vertical face corresponds to the section at a crack; this vertical face is unconstrained and it is this face to which the loads are applied (Figure 10). The stresses applied to the reinforcement bars (σ'_s and σ_s) and to the concrete (σ_c) at the unconstrained face were obtained from the analytical results for a cracked section, obtained from the theoretical analysis described above.

The materials defined in the FE analysis are shown in Figure 11. The properties of the concrete and the reinforcement were obtained experimentally or as quoted in the codes

- 28-day compressive strength of the concrete (‘high-shrinkage’ mix) was 56.7 MPa
- 28-day modulus of elasticity of the concrete was 36.33 GPa
- Poisson’s ratio of the concrete was 0.2

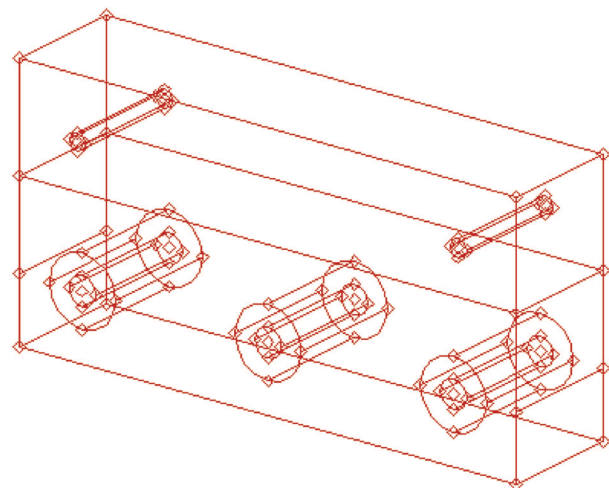


Figure 9. Specimen for FE analysis (300 mm width, 150 mm height, 70 mm length)

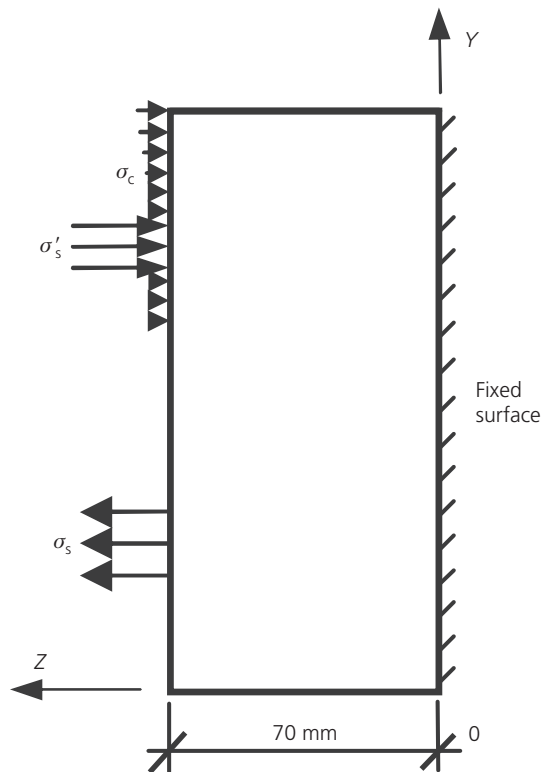


Figure 10. Loads and constraints

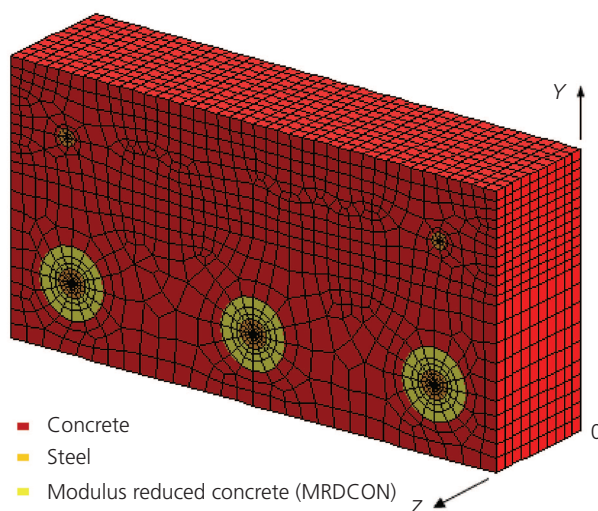


Figure 11. Materials and mesh

- elastic modulus of the steel reinforcement was 210 GPa
- Poisson's ratio of steel was assumed to be 0.3.

To account for secondary (internal) cracks generated in the region around the tensile reinforcement of a crack, a reduced elastic concrete modulus was used for an area 12 of the concrete 12 mm

thick around the reinforcement. This approach has been shown to be representative (Forth and Beeby, 2013). The elastic modulus of this 'special' region of concrete is 14% of the normal concrete.

The static elastic FE analysis was performed on a model representing beam B2 at an age of 90 days. In the analysis, the concrete properties adopted (e.g. strength, modulus of elasticity) and the loads applied were taken from the theoretical analysis described in previous sections. The FE analysis determines the deformation and strain of the specimen. Figure 12 shows the deformation in the Z-direction where it can be seen that the top region is being compressed while the bottom is in tension.

Figure 13 further clarifies the deformation in the Z-direction, illustrating the transition of curvature from the uncracked section (distance = 0 mm) to the cracked section (distance = 70 mm). The curvature plotted in Figure 13 is the resultant shrinkage curvature (i.e. with the elastic curvature removed). The distribution of curvature over the length increases with distance from the uncracked section and the maximum value (occurring near the cracked section) is close to the value for the cracked section obtained from the section analysis. Also shown in Figure 13 is a

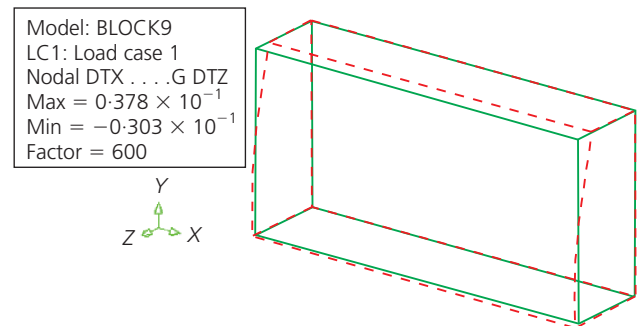


Figure 12. Deformation in the Z-direction

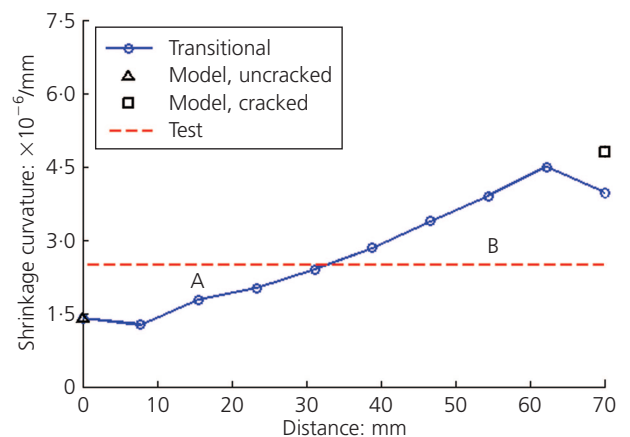


Figure 13. Analysed curvature distribution and mean curvature from tests on B2 at age 90 days

line that represents the experimentally measured mean curvature of beam B2. This line almost equals the average of the curvatures predicted by the FE model from the uncracked to the cracked position (i.e. area *A* almost equals area *B*). From the strain obtained in the FE analysis, the longitudinal curvature of the beam portion can be manually derived. From Figure 13, it is expected that the combined new theoretical and FE models will predict the mean curvature of the experimental beam reasonably well.

4.3 Mean shrinkage curvature

The mean curvature at 90 days calculated for beam B2 using the FE analysis is plotted in Figure 14 along with the curvatures calculated at 30 and 60 days. As can be seen from the figure, the predicted curvature is slightly below that of the experimentally derived curvature, although the trend with time is similar. The shrinkage curvatures of a cracked and uncracked section of the beam as predicted by the proposed theoretical approach are also shown in Figure 14. It can be seen that, in relation to the uncracked and uncracked boundaries, the mean shrinkage curvature is located closer to the uncracked boundary. B2 was loaded to achieve a stabilised crack pattern in the constant-moment zone. In practice, this condition is rarely likely to occur and therefore, for more practical conditions (not fully cracked), the mean curvature is likely to be closer to the uncracked boundary.

Another identical beam pair (B4) was also tested and a similar analysis was performed. A comparison of the measured and predicted mean shrinkage curvatures for this beam is presented in Figure 15. Again, it can be seen that the experimental curvatures were predicted reasonably well. The consistency and accuracy of the measured and predicted shrinkage curvatures suggest that this modelling approach could be used to predict the shrinkage of cracked sections of concrete beams. However, it is necessary to confirm the influence of section size and steel ratio (the beams tested here were designed with a 1.34% reinforcement ratio).

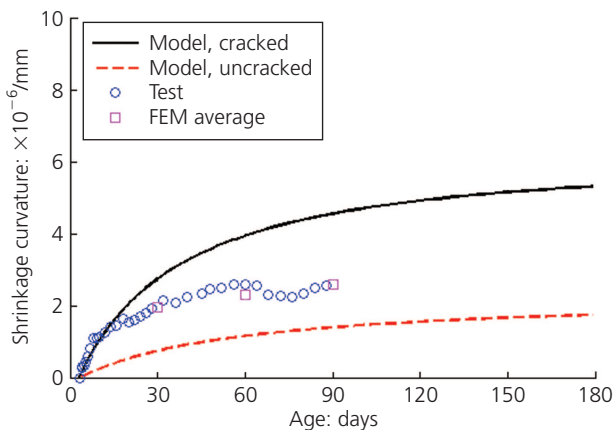


Figure 14. Mean curvatures from FE analysis and test: beam B2

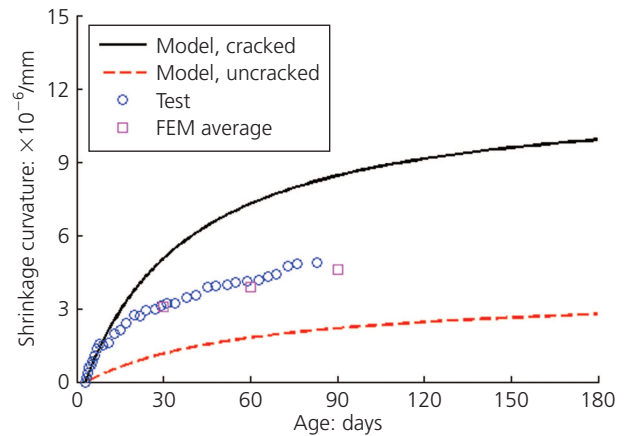


Figure 15. Mean curvatures from FE analysis and test: beam B4

5. Verification of code-predicted mean shrinkage curvatures

Figure 16 compares the shrinkage curvatures derived from codes BS 8110 and EC2 with the theoretical approach proposed in this paper for a cracked section. As explained earlier, the curvature determined according to the code models is exactly the same as that calculated for the new model proposed in this paper for a cracked section. The curvature of an uncracked beam, as predicted by the codes is also provided in Figure 16.

Figure 16 also shows the mean curvature (i.e. combination of the curvatures for cracked and uncracked sections) using Equations 2 and 3. In EC2, it is not clearly explained whether the distribution coefficient ζ should be fixed or should vary with time as σ_s changes due to time-dependent behaviour. Figure 16 therefore presents the EC2 predicted mean curvature with fixed ζ (EC2-mean-fixed) and with variable ζ (EC2-mean-unfixed). Since a variable ζ is considered, reflecting the time-dependent effects, Equation 2 and 3 are also plotted taking $\beta = 1.0$ (so that the

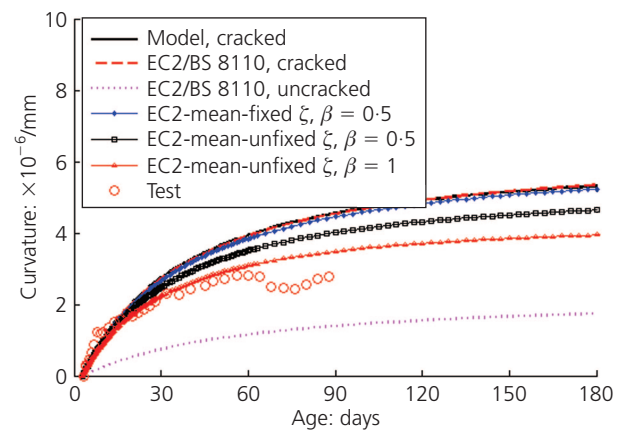


Figure 16. Comparison of shrinkage curvatures

time-dependent effects are not considered twice). From Figure 16 it can be seen that, for the slab-type B2, EC2-mean-unfixed ζ and $\beta = 1$ predicts the curvature reasonably well, particularly at early ages (up to 60 days). However, assuming fixed ζ and $\beta = 0.5$ (for sustained loads), the EC2 equations significantly overestimate the curvature of a cracked beam. Furthermore, beams that are not fully cracked (i.e. those normally found in practice) will possess curvatures that tend towards the uncracked section boundary and, as such, the predictions offered by the codes will be even more conservative.

6. Conclusion

- The analytical approach proposed to calculate the curvature of cracked sections of beams subjected to bending has the following advantages over the models presented in BS 8110 (BSI, 1985) and EC2 (BSI, 2004): the effect of shrinkage and creep are taken into account and approximating using a fixed neutral axis position is unnecessary.
- The proposed model verifies the current code predictions. However, it was found that although the shrinkage curvature predicted by the code models for a cracked section is the same as that obtained with the new approach, this result is fortuitous. This is because applying the shrinkage later reduces the modular ratio and hence reduces I but slightly increases S ; these changes almost exactly balance each other.
- The proposed approach coupled with FE analysis accurately predicted the mean shrinkage curvature of 150 mm deep fully cracked beams with a 1.34% steel ratio. Further investigations are required to confirm that this approach is suitable for deeper beams with a range of steel reinforcement ratios.
- The experimental methodology appears to have been successful in isolating shrinkage curvatures.
- The mean shrinkage curvature of fully cracked beams appears to be overestimated by the models presented in BS 8110 and

EC2 (Equations 1 and 2). However, for this investigation, by considering varying ζ and taking $\beta = 1.0$ (in an attempt not to consider the time-dependent effects twice), the curvature is predicted reasonably well, particularly at early ages.

REFERENCES

- Beeby AW and Scott RH (2004) Insights into the cracking and tension stiffening behaviour of reinforced concrete tension members revealed by computer modelling. *Magazine of Concrete Research* **56(3)**: 179–190.
- BSI (1985) BS 8110-2: 1985: Structural use of concrete. Part 2: Code of practice for special circumstances. BSI, London, UK.
- BSI (2004) BS EN 1992-1-1: 2004: Eurocode 2: Design of concrete structures. Part 1-1: General rules and rules for buildings. BSI, London, UK.
- Faber O (1927) Plastic yield, shrinkage and other problems of concrete and their effects on design. Part 1. *Proceedings of the Institution of Civil Engineers* **225**: 27–73.
- Favre R, Beeby AW, Falkner H, Koprna M and Schiessl P (1983) *Cracking and Deformations. CEB Manual*. Swiss Federal Institute of Technology, Lausanne, Switzerland.
- FIB (Fédération Internationale du Béton) (1993) CIB–FIP Model Code 90. FIB, Lausanne, Switzerland.
- Forth JP and Beeby AW (2013) A study of the composite behaviour of reinforcement and concrete in tension. *ACI Structural Journal*, forthcoming.
- Ghali A and Favre R (1986) *Concrete Structures: Stresses and Deformations*. Chapman & Hall, London, UK.
- Hobbs DW (1979) *Shrinkage-induced Curvature of Reinforced Concrete Members*. Cement and Concrete Association, London, UK.
- Mu R, Forth JP, Beeby AW and Scott R (2008) Modelling of shrinkage induced curvature of cracked concrete beams. In *Tailor Made Concrete Solutions* (Walraven JC and Steelhurst D (eds)). Taylor & Francis, Abingdon, UK, pp. 573–578.

WHAT DO YOU THINK?

To discuss this paper, please email up to 500 words to the editor at journals@ice.org.uk. Your contribution will be forwarded to the author(s) for a reply and, if considered appropriate by the editorial panel, will be published as a discussion in a future issue of the journal.

Proceedings journals rely entirely on contributions sent in by civil engineering professionals, academics and students. Papers should be 2000–5000 words long (briefing papers should be 1000–2000 words long), with adequate illustrations and references. You can submit your paper online via www.icevirtuallibrary.com/content/journals, where you will also find detailed author guidelines.